BRITISH JOURNAL OF HOSPITAL MEDICINE

ARTICLE

A Pathological Prediction Model and Scoring System Including Endoscopic Signs for Duodenal Papilla Neoplasms: A Retrospective Study

Yuting Qiu[1], Yi Yang[1,2], Xinwei Qiao[1], Haobo Li[3], Peng Li[1,*], Jing Wu[1,*], Shutian Zhang[1]

[1]Department of Gastroenterology, Beijing Friendship Hospital, Capital Medical University, Beijing, China
[2]Endoscopy Center, Department of Gastroenterology, Shanghai East Hospital, School of Medicine, Tongji University, Shanghai, China
[3]Graduate School of Peking Union Medical College, Chinese Academy of Medical Sciences, Beijing, China
*Correspondence: lipeng@ccmu.edu.cn (Peng Li); wujing36youyi@ccmu.edu.cn (Jing Wu)

Abstract

Aims/Background The application value of endoscopic ultrasound (EUS) in diagnosing duodenal papilla neoplasms (DPNs) remains underexplored. This study aims to evaluate the role of EUS and other clinical indicators in differentiating between benign and malignant DPNs and to establish a pathological prediction model for DPNs.

Methods Clinical and imaging data of DPNs patients were collected. Least absolute shrinkage and selection operator (LASSO) regression was employed to screen independent predictors. Patients were divided into training and test cohorts. Univariate and multivariate logistic regression analyses were performed. A nomogram was developed alongside a scoring system, both of which were validated using the test cohort.

Results A total of 56 benign and 95 malignant DPNs cases were included. Logistic regression analysis identified age, magnetic resonance imaging (MRI), EUS-measured size, echo intensity and papilla appearance as independent predictors of pathological diagnosis. The nomogram demonstrated a C-index of 0.876, with area under the curve (AUC) values of 0.88 and 0.82 in the training and test cohorts, respectively. The scoring system performed well, with an optimal cutoff value of 14 points.

Conclusion Age, MRI, EUS size and papilla appearance are independent risk factors for malignant DPNs. EUS may have extraordinary effects in DPNs differential diagnosis.

Key words: nomograms; duodenal neoplasms; endosonography; ampulla of vater

Submitted: 28 August 2024 Revised: 10 December 2024 Accepted: 18 December 2024

Introduction

The common bile duct and the main pancreatic duct converge at the ampulla in most individuals, opening into the duodenum at the major duodenal papilla (MDP). The MDP is a unique anatomical region that is constantly exposed to chemical and mechanical stimulation (Panzeri et al, 2015). Duodenal papilla neoplasms (DPNs) are a significant subset of ampullary tumors. Epidemiological surveys indicate that ampullary cancer is most prevalent in individuals aged 50 to 70 years, with an age-adjusted incidence rate of 0.70 per million in men and 0.45 per million in women (Meijer et al, 2020). Given the unique anatomical location of the lesion, patients with DPNs often present with obstructive symptoms early in the disease, enabling

How to cite this article:
Qiu Y, Yang Y, Qiao X, Li H, Li P, Wu J, Zhang S. A Pathological Prediction Model and Scoring System Including Endoscopic Signs for Duodenal Papilla Neoplasms: A Retrospective Study. Br J Hosp Med. 2025. https://doi.org/10.12968/hmed.2024.0585

detection of tumors at a very small size, which can be surgically resected for favorable prognoses. However, in the early stages, even malignant lesions may lack distinct malignant features, making them challenging to be differentiated from benign lesions.

The current treatment options for DPNs primarily include endoscopic papillectomy (EP), transduodenal ampullectomy (TDA), and pancreaticoduodenectomy (PD) (Nappo et al, 2020). The choice of treatment significantly impacts patient prognosis, with pathological diagnosis serving as a crucial determinant in guiding therapeutic decisions. Pathological findings influence both the complete lesion removal and the risk of recurrence (Li et al, 2019; Lian et al, 2017). For DPNs, however, there is a notably low concordance between the histomorphological grading of endoscopic biopsy specimens and those obtained after papillectomy (Haraldsson et al, 2015; Kawashima et al, 2021).

Clinically, the evaluation of DPNs often requires the combination of magnetic resonance imaging (MRI), computed tomography (CT), endoscopic ultrasound (EUS), and other examination methods (Kandler and Neuhaus, 2018). EUS is currently widely recommended for the diagnosis of DPNs. By positioning the probe in close proximity to the duodenal wall, EUS provides direct visualization of the lesion. It not only has a great sensitivity in lesion screening, but can also accurately define the infiltration of surrounding tissues, and has a high accuracy rate in predicting T staging. Furthermore, EUS has comparable performance to endoscopic retrograde cholangiopancreatography (ERCP) in evaluating ampullary lesions associated with ductal dilatation, while offering greater safety (Gaspar and Shami, 2015; Panzeri et al, 2015; Ridtitid et al, 2015). However, the specific impact of EUS on preoperative evaluation of DPNs hasn't been fully elucidated, and there is ongoing debate regarding the optimal timing and indications for its use in DPN assessment (Peng et al, 2019).

In this study, we investigated independent predictive factors for DPNs and developed a pathological prediction model and scoring system to evaluate the pathological outcomes of DPNs.

Methods

Patients

We retrospectively searched patients with DPN who were admitted to Beijing Friendship Hospital, Capital Medical University, and received endoscopic or surgical treatment from 2015 to 2022. Inclusion criteria: (a) The MDP was the primary site of tumor or the ampullary location of the primary tumor involving the MDP; (b) Patients had not received adjuvant therapies, such as chemotherapy or radiotherapy, prior to undergoing EUS examination and treatment. We initially collected 181 patients diagnosed with ampullary or duodenal papilla carcinoma. Among them, 13 patients gave up final treatment, which referred to endoscopic resection or surgical intervention for the lesion, resulting in the absence of final pathological results. 5 patients did not receive EUS examination before treatment, and 12 patients had $\geq$20% missing clinical data and were ultimately excluded from the study (Fig. 1).

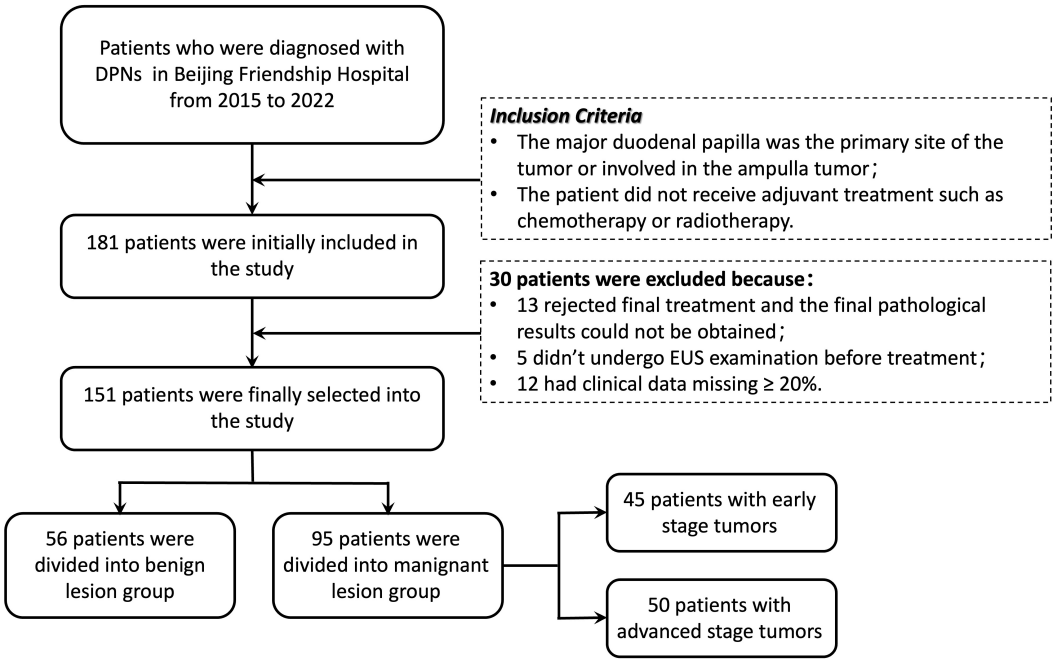

Fig. 1. Flow diagram of the enrolled patients. The figure was created by Microsoft PowerPoint 2021 (Microsoft Corporation, Redmond, WA, USA). DPNs, duodenal papilla neoplasms; EUS, endoscopic ultrasound.

Data Acquisition

EUS

All EUS examinations were performed by experienced endoscopists in Beijing Friendship Hospital using echoendoscopes GF-UE260-AL5 or GF-UCT260 (Olympus, Tokyo, Japan) and/or EG-3670URK, EG-3270UK or EG-3870UTK (Pentax, Tokyo, Japan). The EUS-related indicators included in this study were as follows: (1) EUS size: represented by the longest diameter of the lesion under EUS, the lesion was divided into three groups: (a) $<$1.0 cm; (b) $\geq$1.0 cm but $<$2.4 cm; (c) $\geq$2.4 cm; (2) Echo intensity: the lesion was divided into an/hypo-echoic and iso/hyper-echoic groups (Fig. 2A,B); (3) Echo uniformity: homogeneous and heterogeneous echo uniformity (Fig. 2C,D); (4) Invasion: the lesions were confined to the submucosa or broke through the submucosa (Fig. 2E,F); (5) Papillary appearance: (a) There may be no obvious abnormality in papillary morphology, with only minor changes such as mucosal redness; (b) Mild deformation, including swelling, mild erosion, etc. (c) Severe deformation, including severe erosion, ulcers and even cauliflower-like changes (Fig. 2G,H). All patients in this study had EUS examination by the same endoscopist with more than 2000 cases of EUS operation experience in Beijing Friendship Hospital.

CT/MRI

The CT results included abdominal plain and enhanced CT scans, while the MRI results comprised plain and enhanced MRI or magnetic resonance cholangiopancreatography (MRCP). Positive findings described as following in the report could guide the patient for further endoscopy examination: abnormal duodenal

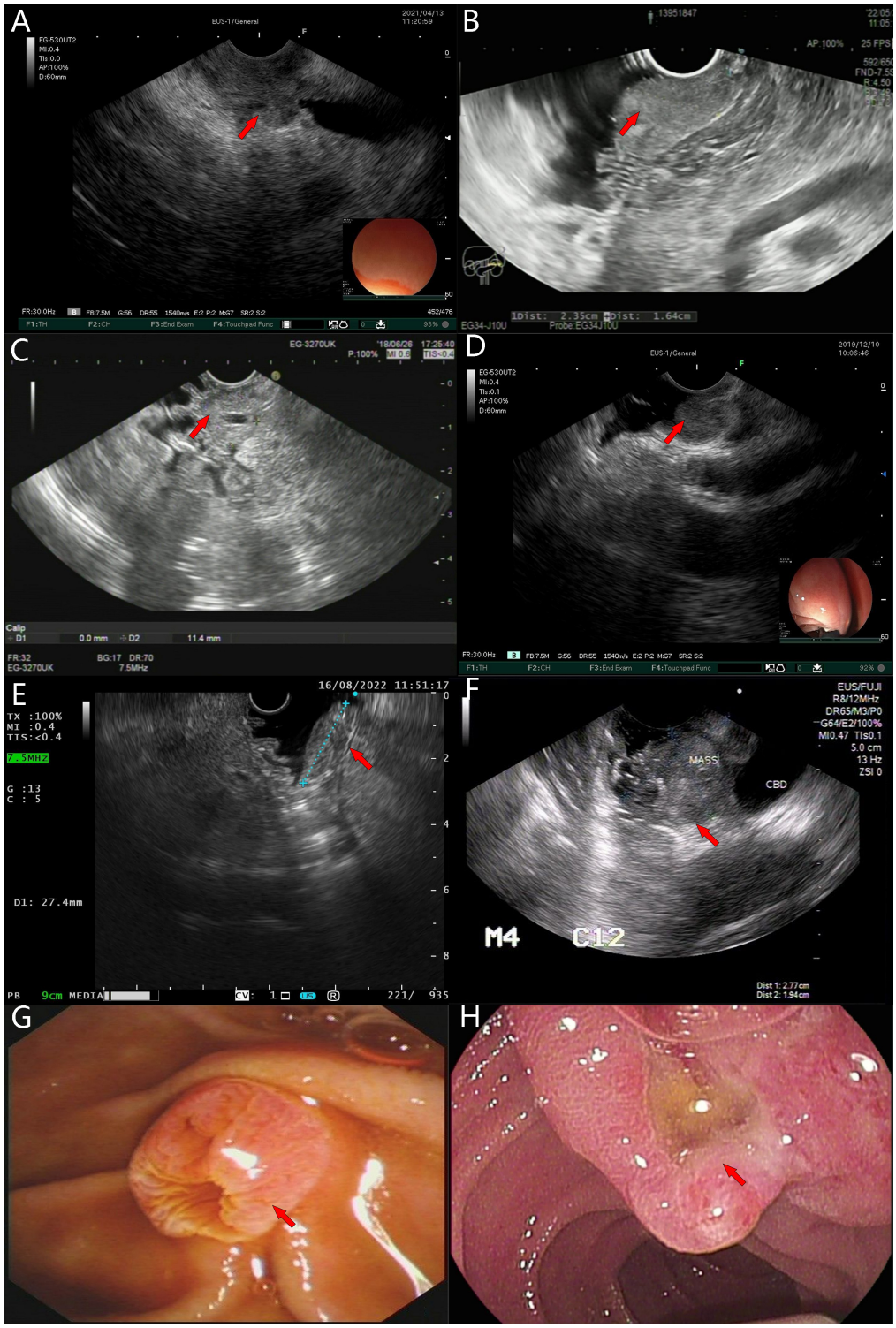

Fig. 2. Different manifestations of DPN lesions under endoscopy and EUS. (A) Hypo-echoic lesion. (B) Iso/hyper-echoic lesion. (C) Lesion with homogeneous echo uniformity. (D) Lesion with heterogeneous echo uniformity. (E) Lesion with a clear boundary and an intact submucosa. (F) The muscularis of the lesion is unclear, involving the distal segment of bile duct and pancreatic duct. (G) Papilla with mild deformation. (H) Papilla presented dished protrusion with ulceration in the center. The red arrows show the lesion areas.

papilla with a size >1 cm in diameter (Dusunceli Atman et al, 2015); presence of nodules or masses in the duodenal papilla or ampullary area; or irregular duodenal papillary appearance. Abnormal bile and pancreatic duct with bile duct diameter >1.2 cm or pancreatic duct diameter >3 mm (Wang et al, 2021); or thickening of the wall of the lower common bile duct.

General Characteristics of the Patients

This part of the data includes gender, age, symptoms, disease history (familial adenomatous polyposis (FAP), cancer, hypertension (HT), diabetes mellitus (DM), coronary heart disease (CHD)), personal history (smoking, alcohol, height, weight, body mass index (BMI)), and family history (cancer). Two situations where patients visiting the hospital are: (a) duodenal papilla abnormality found by physical examination, and (b) clinical symptoms such as fever, abdominal pain, jaundice and anorexia occur. Patients in situation (a) was classified as asymptomatic group.

Laboratory Tests

The part of the index is divided into four parts: (a) Tumor biomarkers (alpha fetoprotein (AFP), carcinoembryonic antigen (CEA), carbohydrate antigen 19-9 (CA19-9), carbohydrate antigen 125 (CA125) and carbohydrate antigen 72-4 (CA72-4), carbohydrate antigen 50 (CA50), neuron specific enolase (NSE), cytokeratin 19 fragment (CYFRA211)); (b) The biochemical indicators (alanine aminotransferase (ALT), aspartate aminotransferase (AST), alkaline phosphatase (ALP), γ-glutamyl transferase (GGT), total bilirubin (TBIL), direct bilirubin (DBIL), indirect bilirubin (IBIL)); (c) Routine blood indicators (white blood cell (WBC), granulocyte% (GR%), hemoglobin (HB), platelet (PLT)); (d) Other relevant indicators (C-reactive protein (CRP), urine bilirubin (UBIL), occult blood (OB)). Due to the high proportion of missing values, CA72-4, CA50, CRP and other indicators were transformed into categorical variables. The cutoff values of the three indicators were 8.2 U/mL and 25 U/mL, and 8 mg/L, respectively, which are criteria values of these indicators in laboratory department in Beijing Friendship Hospital.

Pathologic Classification

Pathologic classification included inflammatory lesions, adenomatous lesions and carcinomas. For adenomas, the final pathological classification was divided into low grade intraepithelial neoplasia (LGIN), high grade intraepithelial neoplasia (HGIN) according to the 2010 World Health Organization (WHO) classification of tumors of digestive system (Nagtegaal et al, 2020). The main pathological type of papilla cancer was adenocarcinoma, regardless of the degree of differentiation, origin and morphology.

Statistics Analysis

Continuous variables with normal distribution were expressed as Mean ± standard deviation (Mean ± SD), and the differences between benign and malignant groups were compared by independent sample *t* test. The continuous variables with non-normal distribution were expressed as median and interquartile range (Q1, Q3) and analyzed by Mann-Whitney U test. Categorical variables were expressed

as percentages and analyzed by chi-square test. Shapiro-Wilk test was used for the normality testing. Different chi-square test methods were selected according to the sample size and the theoretical frequency (T) of each index. When the sample size >40 and T >5, Pearson's chi-square test was selected, and when the above conditions were not met or there were non-dichotomous variables, Fisher's exact test was selected. Spearman correlation analysis was used to analyze the correlation between each variable and correlation heat map was generated. The mutual independent indicators were screened by least absolute shrinkage and selection operator (LASSO) regression to predict the clinical factors related to pathological results. Patients were randomly divided into training and test set in an 8.5:1.5 ratio. Univariate and multivariate logistic regression analysis were conducted to screen out the independent predictive factors, and then the nomogram was drawn. The predictive accuracy of the nomogram was assessed using the receiver operating characteristic (ROC) curve, and the area under the curve (AUC) was calculated. Calibration and decision curve analyses (DCA) were conducted to evaluate the model's performance based on patients in training set. In addition, the malignant group was further divided into early-stage and advanced-stage carcinoma groups, and the same analytical approach was applied to identify relevant predictive factors. Inspired by Ben AH's study (Ben Ayed et al, 2019), we used the regression coefficients of each independent predictor to further establish a scoring system. We divided the coefficient of each index by 1/2 of the minimum coefficient of the quantitative index, and the nearest integer value is the score of the index.

In terms of missing clinical data of some patients, if the missing percentage was less than 10%, MissForest algorithm was used to fill in the missing value. When missing percentage was more than 10%, a new grouping called Unknown were created. $p < 0.05$ was considered statistically significant except for logistic regression of benign and malignant duodenal papillary neoplasms, in which $p < 0.1$ was considered statistically significant. All the above analyses were implemented using R 4.4.2 (R Foundation for Statistical Computing, Vienna, Austria).

Results

A total of 151 patients were included in the final analysis, comprising 56 (37.1%) patients with benign DPNs and 95 (62.9%) with malignant DPNs. There were no significant differences in gender between the two groups. The mean age of all patients was 59.03 ± 11.44 years, with 54.79 ± 10.98 years in the benign group and 61.54 ± 11 years in the malignant group. Significant differences were observed in age, height and symptom between the two groups in the baseline data. Factors such as family history of cancer, and FAP did not differ significantly between the two groups (**Supplementary Table 1**). Significant differences were noted in overall tumor biomarkers between the groups, including CEA, CA125, CA19-9, and CA50, which were markedly elevated in the malignant group. The levels of transaminase and bilirubin in the malignant group were significantly higher than those in the benign group. There were also differences in the levels of GR%, HB, CRP and UBIL in the routine blood test, while there was no difference in OB (**Supplementary Ta-**

Table 1. Imaging characteristics of patients of benign and malignant duodenal papillary neoplasms.

Variables	Benign (n = 56)	Malignant (n = 95)	z	χ^2	*p* value
CT				13.39	0.001**
Negative	19 (33.9)	14 (14.7)			
Positive	24 (42.9)	69 (72.6)			
Unknown	13 (23.2)	12 (12.6)			
MRI				24.96	<0.001***
Negative	14 (25.0)	10 (10.5)			
Positive	13 (23.2)	62 (65.3)			
Unknown	29 (51.8)	23 (24.2)			
EUS size	1.47 (1.0, 1.83)	2.00 (1.59, 2.60)	5.306		<0.001***
Invasion				29.06	<0.001***
Within submucosa	51 (91.2)	45 (47.4)			
Breakthrough submucosa/metastasis	5 (8.9)	50 (52.6)			
Echo intensity				11.33	0.004**
Non/hypo-echoic	22 (39.3)	61 (64.2)			
Iso/hyper-echoic	15 (26.8)	9 (9.5)			
Unknown	19 (33.9)	25 (26.3)			
Echo unifomity				2.08	0.354
Homogeneous	15 (26.8)	19 (20.0)			
Heterogeneous	10 (17.9)	26 (27.4)			
Unknown	31 (55.4)	51 (53.7)			
Papilla appearance				18.57	<0.001***
Mild abnormal	32 (57.1)	25 (26.3)			
Mild deformation	20 (35.7)	40 (42.1)			
Severe deformation	2 (3.6)	15 (15.8)			
Unknown	2 (3.6)	15 (15.8)			

Categorical variables are presented as frequencies and percentages. Continuous variables are presented as median (inter-quartile range). **$p < 0.01$, ***$p < 0.001$. CT, computed tomography; MRI, magnetic resonance imaging; EUS, endoscopic ultrasound.

ble 2). Regarding imaging examination, the median size of the benign lesion group was 1.47 cm, and that of the malignant lesion group was 2.00 cm, which was significantly different. In addition, except for the echo uniformity, CT, MRI and other EUS indicators demonstrated diagnostic potential (Table 1).

In addition, the ranking of the AUC of indices which are significantly different between two groups is shown in the bar chart in Fig. 3A. Among these indicators, the top three with relatively high diagnostic value are EUS size, Tumor biomarkers and AST. However, the highest AUC was only 0.76, indicating that the diagnostic performance of any single index in distinguishing between benign and malignant DPNs is limited. Therefore, the value of single index in judging the benign and malignant DPN is limited. Although most of the indicators we included were significantly different between the two groups, the correlation heat map (Fig. 3B) revealed significant intercorrelations among them. LASSO regression analysis was

conducted to reduce collinearity and screened out age, AST, GGT, TBIL, HB, MRI, EUS size, echo intensity and papilla appearance to be included in the logistic regression analysis (Fig. 3C,D).

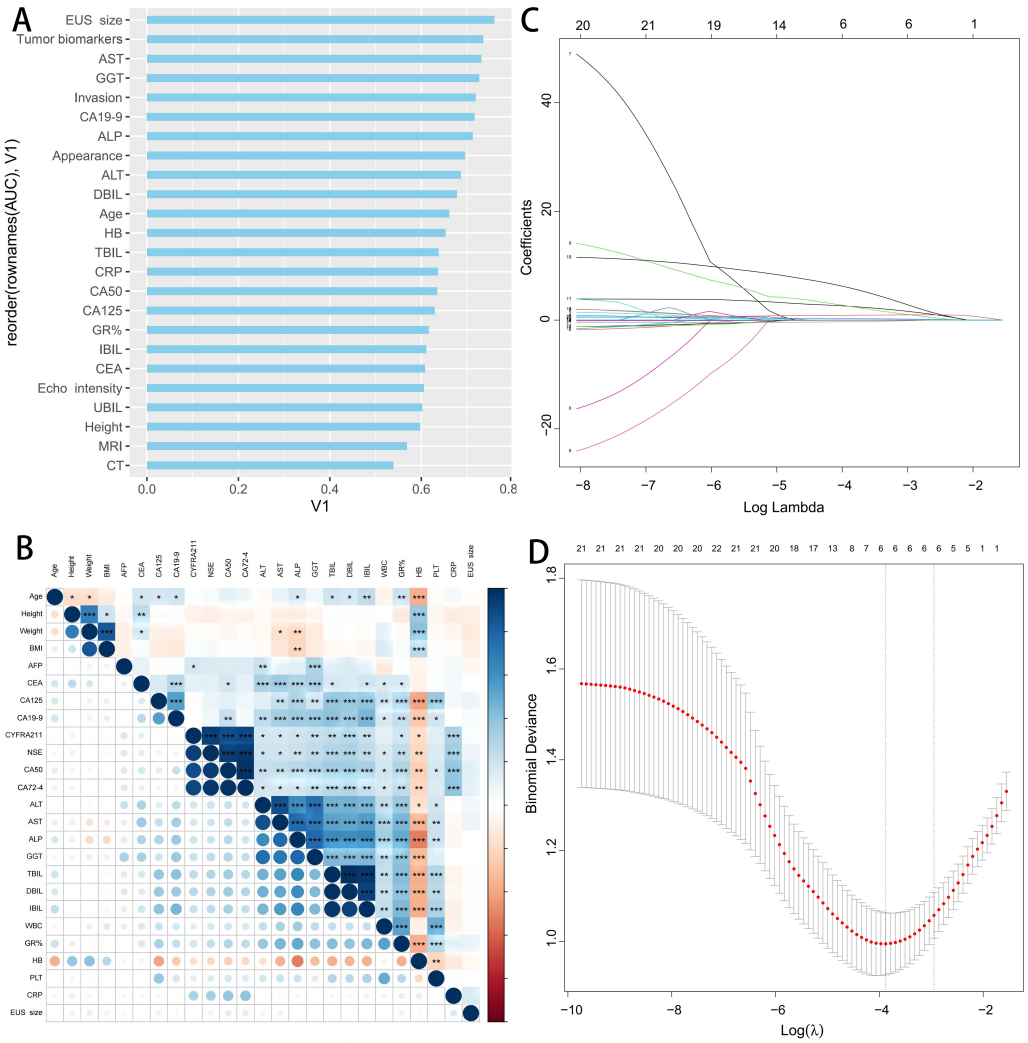

Fig. 3. Variables selection for construction of pathological prediction model. (A) Sort the AUC bar chart of indices which are significantly different between two groups for identifying benign and malignant lesions using individual indicators. (B) Correlation heatmap between variables. *$p <$ 0.05, **$p < 0.01$, ***$p < 0.001$. (C) Profiles of LASSO coefficients. (D) LASSO coefficient values of indicators with discriminative value. AUC, area under the curve, LASSO, least absolute shrinkage and selection operator; AST, aspartate aminotransferase; GGT, γ-glutamyl transferase; CA19-9, carbohydrate antigen 19-9; ALP, alkaline phosphatase; ALT, alanine aminotransferase; DBIL, direct bilirubin; HB, hemoglobin; TBIL, total bilirubin; CRP, C-reactive protein; CA50, carbohydrate antigen 50; CA125, carbohydrate antigen 125; GR%, granulocyte%; IBIL, indirect bilirubin; CEA, carcinoembryonic antigen; UBIL, urine bilirubin; BMI, body mass index; AFP, alpha fetoprotein; CYFRA211, cytokeratin 19 fragment; NSE, neuron specific enolase; CA72-4, carbohydrate antigen 72-4; WBC, white blood cell; PLT, platelet.

There are 128 patients (48 with benign lesions and 80 with malignant lesions) in training set and 23 patients (8 with benign lesions and 15 with malignant lesions)

in test set. In the training set, univariate logistic regression showed that age, MRI, EUS size and papilla appearance remained significantly different between the two groups ($p < 0.1$). Given the apparent importance of imaging features in differentiating benign from malignant tumors, echo intensity was included in the multivariate logistic regression analysis and the establishment of the nomogram as well. Multivariate logistic regression confirmed that all the five indicators included were independent predictors of benign and malignant lesions with $p < 0.1$. Among them, echo intensity was negatively correlated with pathological results, with an/hypoecho intensity more commonly associated with malignant lesions. Increased age, positive MRI, increased EUS size, and abnormal papillary appearance were independent risk factors for malignant lesions (Table 2). The C index of the model is 0.876 and the nomogram is presented in Fig. 4A. The model achieved an AUC of 0.88 (95% confidence interval (CI): 0.81–0.94, $p < 0.001$) in the training group, with a sensitivity of 81.3% and specificity of 85.4%, indicating excellent diagnostic efficiency for DPNs (Fig. 4B). In the test group, the AUC was 0.82 (95% CI: 0.59–1.00, $p = 0.005$), with a sensitivity of 100% and specificity of 62.5%, further validating the diagnostic performance of the model (Fig. 4C). Additionally, there were no significant differences in AUC between the training and test sets ($p > 0.05$), suggesting comparable model performance in both datasets. The calibration curve and DCA also highlighted the practical application value of the model (Fig. 4D,E).

We established a simple scoring system to facilitate the application in clinical practice. The coefficient of each categorical variable was divided by half the minimum coefficient (0.6) to calculate the corresponding scores. For age, which was included in the multivariate logistic regression as a continuous variable, we also divided its coefficient by 0.6 and multiplied the result by the age value to derive the score (Table 3). We subsequently tested the scoring system on a subset of 50 patients to determine the optimal cutoff value for differentiation. The diagnostic efficacy of some cutoff values was shown in **Supplementary Table 3**. The sensitivity, specificity, positive predictive value (PPV), negative predictive value (NPV) and accuracy of the scoring system were 91.4%, 86.7%, 94.1%, 90% and 90%, respectively, when the cutoff value was 14 points. Notably, this scoring system serves as an extension of the nomogram and shows no substantial differences in diagnostic performance.

We further divided the patients in the malignant group into early-stage carcinoma (45, 47.4%) and advanced-stage carcinoma (50, 52.6%). The mean age of the two groups was 60.89 $\pm$ 10.3 years and 62.12 $\pm$ 11.67 years, respectively, with no significant difference. LASSO regression was performed to identify mutually independent indicators for inclusion in the logistic regression analysis (**Supplementary Fig. 1**). There was a significant difference in the symptoms between the two groups (**Supplementary Tables 4–6**). Patients with advanced cancer were more likely to present with symptoms such as jaundice, fever, and abdominal pain. Finally, it was found that the presence of symptoms, GGT level and CA50 level were independent predictive factors for the differentiation of early- and advanced-stage DPNs (Table 4). However, there were no significant differences in imaging factors including

Table 2. Univariate and multivariate logistic regression analysis of benign and malignant duodenal papillary neoplasms.

Variables	Univariate logistic regression						Multivariate logistic regression					
	β	Wald Z	S.E.	OR	90% CI	p value	β	Wald Z	S.E.	OR	90% CI	p value
Age	0.046	1.910	0.024	1.047	1.007–1.090	0.056*	0.051	2.410	0.021	1.052	1.016–1.090	0.016*
AST	0.020	0.660	0.031	1.021	0.970–1.074	0.509						
GGT	0.003	0.770	0.004	1.003	0.997–1.009	0.439						
TBIL	0.005	0.270	0.019	1.005	0.974–1.037	0.790						
HB	–0.003	–0.150	0.019	0.997	0.967–1.029	0.880						
MRI												
Positive	2.101	2.480	0.848	8.177	2.027–32.997	0.013*	2.260	3.050	0.742	9.586	2.829–32.484	0.002**
EUS size												
≥1.0 cm, <2.4 cm	1.665	1.980	0.843	5.287	1.322–21.145	0.048*	1.746	2.170	0.803	5.728	1.528–21.475	0.030*
≥2.4 cm	2.273	2.130	1.065	9.708	1.684–55.970	0.033*	2.645	2.610	1.013	14.083	2.659–74.576	0.009**
Echo intensity												
Iso/hyper-echoic	–0.939	–1.240	0.757	0.391	0.113–1.357	0.215	–1.226	–1.690	0.724	0.294	0.089–0.966	0.090*
Papilla appearance												
Mild deformation	1.063	1.760	0.604	2.893	1.071–7.815	0.079*	1.262	2.170	0.582	3.531	1.357–9.193	0.030*
Severe deformation	0.714	0.600	1.186	2.042	0.290–14.365	0.547	1.854	1.750	1.060	6.388	1.118–36.498	0.080*

*$p < 0.1$, **$p < 0.01$. S.E., Standard Error; OR, odds ratio; CI, confidence interval; AST, aspartate aminotransferase; GGT, γ-glutamyl transferase; TBIL, total bilirubin; HB, hemoglobin; MRI, magnetic resonance imaging; EUS, endoscopic ultrasound.

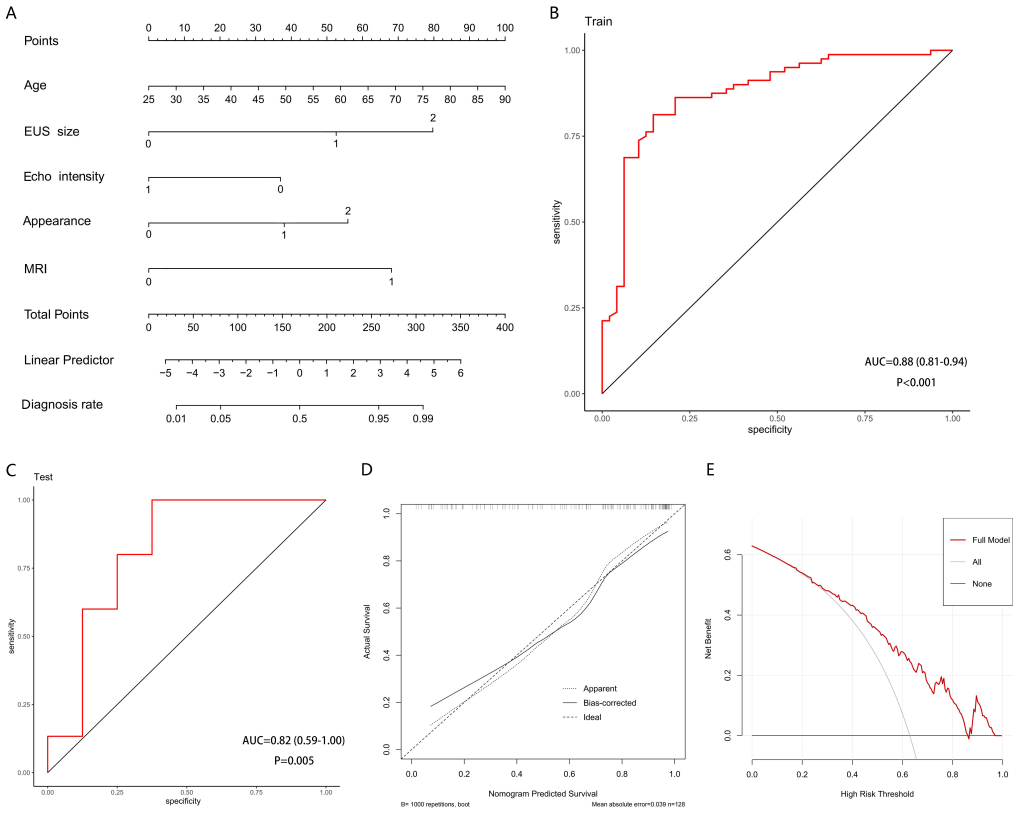

Fig. 4. Construction and validation of the nomogram for DPNs. (A) Nomogram predicting the pathological results of duodenal papillary neoplasms. Meaning of numbers "0", "1" and "2" for each categorical variable. EUS size: "0"—<1.0 cm; "1"—≥1.0 cm but <2.4 cm; "2"—≥2.4 cm. Echo intensity: "0"—an/hypo-echoic; "1"—iso/hyper-echoic groups. Appearance: "0"—Normal; "1"—Mild deformation; "2"—Severe deformation. MRI: "0"—positive; "1"—negative. (B) The ROC curve analysis based on the nomogram in training group. (C) The ROC curve analysis based on the nomogram in testing group. (D) Calibration plots for assessing the consistence between the predicted and the actual diagnostic rate for the nomogram based on patients in training set. (E) Decision curve analysis of the pathological prediction model based on patients in training set. MRI, magnetic resonance imaging; ROC, receiver operating characteristic.

CT, MRI and EUS indicators between the two groups, which was contrary to that in benign and malignant groups.

Discussion

In this study, we identified age, MRI, EUS size, echo intensity, and papilla appearance as independent predictors of benign and malignant DPNs, and plotted a nomogram and a scoring system for pathological prediction. With a cutoff value set at 14, the system expressed ideal sensitivity, specificity, PPV, NPV and accuracy.

Previous studies have explored the non-invasive imaging characteristics and other clinical factors of DPNs, and developed relevant nomogram or scoring system (Dusunceli Atman et al, 2015; Jang et al, 2021; Sun et al, 2013; Wang et al, 2021). Wang et al (2021) found that DBIL elevation >7 umol/L, pancreatic duct dilatation >5 mm, and irregular papilla shape were significantly correlated with

Table 3. A score system of pathological results of duodenal papilla neoplasms.

Variables	Score
MRI	
-	0
+	4
EUS size	
$<$1.0 cm	0
1.0 $\leq$ x $<$ 2.4 cm	3
x $\geq$2.4 cm	4
Echo intensity	
An/hypo-echoic	2
Iso/hyper-echoic	0
Papilla appearance	
Regular	0
Mild deformation	2
Severe deformation	3
Age	1/12 $\times$ Age

MRI, magnetic resonance imaging; EUS, endoscopic ultrasound.

Table 4. Multivariate logistic regression analysis of early-stage and advanced duodenal papillary lesions.

Variables	β	S.E.	Wald	OR	95% CI	p value
Symptom	–1.233	0.604	4.173	0.291	0.089–0.951	0.041*
CA125	0.076	0.044	2.961	1.079	0.990–1.176	0.085
CA50						
$\leq$25 U/mL	–1.663	0.481	11.945	0.190	0.074–0.487	0.001**
$>$25 U/mL	–2.464	1.582	2.427	0.085	0.004–1.889	0.119
GGT	0.003	0.001	7.447	1.003	1.001–1.005	0.006**
TBIL	0.000	0.006	0.005	1.000	0.988–1.011	0.943

*$p < 0.05$, **$p < 0.01$. S.E., Standard Error; OR, odds ratio; CI, confidence interval.

malignant lesions. The scoring system achieved a sensitivity of 78.8% and a specificity of 88.1% (Wang et al, 2021). In addition, Jang SY's team (2021) established a nomogram incorporating CT signs to predict ampullary malignancy, including the presence and size of masses, total bilirubin level and age. In terms of EUS, Rejeski JJ's team (2016) enrolled 50 patients and identified size, tissue infiltration, pancreatic duct dilatation, T stage, lymph node involvement, and catheter stent placement as factors enhanced risk stratification and more precise screening of patients suitable for treatment.

The value of age in differentiating benign from malignant DPNs has been highlighted in many studies (Jang et al, 2021; Li et al, 2019). In terms of non-invasive imaging procedures, our study found that the diagnostic value of MRI was superior to that of CT, despite the well-documented utility of CT in diagnosing DPNs (Nikolaidis et al, 2014; Wei et al, 2023). This discrepancy may be attributed to our focus

solely on final CT results. However, prior studies have noted that the diagnostic accuracy of abdominal CT is relatively low for small lesions, especially masses located within the duodenal wall. Moreover, the accuracy depends on the state of duodenal expansion (Ivanovic et al, 2017; Panzeri et al, 2015). There is no doubt about the diagnostic value of MRI, especially MRCP, in biliopancreatic lesions. Features such as focal wall thickening, invasive annular stenosis, and intramural or intraductal polypoid masses are characteristic MRI findings of ampullary lesions (Dusunceli Atman et al, 2015; Nikolaidis et al, 2014). However, the ampullary region is sometimes called the "blind spot" of MRI due to the small volume of the ampulla and insufficient fluid volume due to the narrowing of the canal. Compared with EUS, MRI can detect ampullary tumors in only 3/4 cases (Panzeri et al, 2015).

Previous studies on DPNs have shown that the size of malignant lesions is significantly larger than that of benign adenomas, and lesions $\geq$2 cm are more likely to be cancerous (Haraldsson et al, 2015; Li et al, 2019). Moreover, high-grade adenomas were significantly larger than low-grade adenomas (Hijikata et al, 2017). In this study, two cutoff values of DPNs size, 1.0 cm and 2.4 cm, were set, with different lesion sizes assigned corresponding scores. It contributed to predicting the benign and malignant lesions more accurately. Papilla appearance is of great significance and has important value in the diagnosis and treatment of many diseases of the digestive system (Balan et al, 2020; Chen et al, 2020; Wang et al, 2021). If the lesion is slightly elevated, the surface appearance is regular, soft and without ulceration, it is more likely to be a benign lesion, while if the lesion is firm and/or ulcerated with spontaneous bleeding, it tends to be a malignant one (Kandler and Neuhaus, 2018).

Certain indicators hypothesized to be associated with DPNs were not included in the final predictive model, such as clinical symptoms, FAP history, bilirubin level, transaminase, tumor biomarkers, and invasion under EUS. In terms of clinical symptoms, previous studies found that there was no difference in abdominal pain and fever between benign and malignant lesions, while jaundice was a more valuable clinical manifestation (Li et al, 2019; Wei et al, 2023). Although clinical symptoms were not incorporated into the scoring system in our study, they emerged as independent predictors in the subgroup analysis differentiating early and advanced carcinomas. FAP is also recognized to be associated with a high risk of developing ampullary neoplasms, with a 124-fold increased risk compared to the general population (Komori et al, 2016; Mehta et al, 2021). Our study did not find an association between FAP and benign or malignant DPN, possibly due to the limited number of FAP patients in the cohort, with only two patients only two cases in each group. It is also plausible that while FAP increases the prevalence of ampullary tumors, it may not directly influence their pathological stages. Bilirubin and transaminase levels, especially TBIL, DBIL, GGT and ALP, which are related to biliary obstruction, did not appear in the prediction model (Wei et al, 2023), but GGT is indeed an independent risk factor for the differentiation of early and advanced stages of malignant DPNs. With regard to tumor biomarkers, previous studies have shown that there is a significant difference in the level of CA19-9 between benign and malignant lesions (Wei et al, 2022; Wei et al, 2023). In our study, although multiple tumor

markers, including CA19-9, were different between benign and malignant lesions in the preliminary correlation analysis, they were not independent risk factors. Interestingly, CA50, rather than CA19-9, CA125, etc., was identified as one of the independent risk factors for differentiating malignant lesions in the subgroup analysis. Invasion has been associated with Tumor/Node/Metastasis staging in duodenal papillary carcinoma (Lian et al, 2017), but it was not included in this model. This may be due to the limitations of EUS, which has high accuracy (98%–100%) for T1 lesions but reduced accuracy for T2, T3, and T4 lesions (Peng et al, 2019). In our study, it can also be found that imaging examination may play an important role in the differentiation of benign and malignant DPNs. When the focus shifts to the differentiation of early and advanced stages of malignant lesions, imaging results are less critical, and clinical symptoms, tumor biomarkers and transaminase levels assume greater importance.

This study has the following limitations: Firstly, as a retrospective study, it is prone to selection bias and provides a lower level of evidence; Secondly, DPN was a relatively rare clinical condition, making it challenging to increase the sample size. Therefore, we had to set the significance threshold to 0.1 in logistic regression model of benign and malignant groups in order to improve the model parameterization and testing performance. Due to the same reason, the nomogram and scoring system were not externally validated, and their clinical application value requires further verification. Thirdly, EUS indicators included in this study were limited. In future studies, biliopancreatic duct status, lymph node metastasis, and white opaque substance (WOS) can be further included (Fukusada et al, 2021; Luchini et al, 2016; Prenzel et al, 2014; Wei et al, 2023). Fourthly, this study only shallowly divided the lesions into benign and malignant ones, without considering more specific pathological types.

Conclusion

This study demonstrated that imaging features play a crucial role in distinguishing between benign and malignant DPNs. A clinicopathological prediction model and scoring system, incorporating indicators such as age, MRI, EUS size, echo intensity, and papilla appearance, was developed and exhibited excellent diagnostic accuracy. This model could address the limitations associated with the relatively low diagnostic efficiency of biopsy for DPN lesions, providing a more reliable prediction of the pathological type of lesions prior to surgery. Additionally, we found that, in differentiating between early and advanced stages of malignant DPNs, clinical symptoms, tumor biomarkers, and transaminase levels were more significant than imaging findings.

Key Points

- The pathological results of duodenal papilla neoplasms (DPNs) have an important influence on treatment and prognosis.
- Imaging features of different methods, especially of endoscopic ultrasound (EUS), are valuable for differentiation of benign and malignant DPNs.
- Age, magnetic resonance imaging (MRI), EUS size, echo intensity and papilla appearance are independent predictors of benign and malignant DPNs.
- The clinicopathological prediction model and scoring system have an ideal diagnostic accuracy for DPNs differential diagnosis and may make up for the deficiency of low diagnostic efficiency of biopsy to a certain extent.
- Presence of symptoms, GGT level and CA50 level play more important roles than imaging manifestation in differentiation of early- and advanced-stage malignant DPNs.

Availability of Data and Materials

All data used during the study are available from the corresponding authors on reasonable request.

Author Contributions

Study conception and design: PL, JW, SZ; EUS performance: PL, JW, SZ; acquisition of data: YQ, XQ, HL; analysis and interpretation of results: YQ, YY; draft manuscript: YQ, YY, HL, XQ; critical revision: all of the authors. YQ and YY contributed equally to the article. All authors reviewed the results and approved the final version of the manuscript. All authors agreed to be accountable for all aspects of the work in ensuring that questions related to the accuracy or integrity of any part of the work are appropriately investigated and resolved.

Ethics Approval and Consent to Participate

The study included human subjects was approved by Ethics Committee of Beijing Friendship Hospital, Capital Medical University with approval number 2022-P2-044-02, and was conducted according to the tenets of the Declaration of Helsinki. Written informed consent was obtained from the proxy of the patients.

Acknowledgement

We thanked Wenkun Li from Department of Gastroenterology, Beijing Friendship Hospital, Capital Medical University, for his critical suggestion on data and statistical methodologies in this research.

Funding

This work was supported by National Natural Science Foundation of China (82070575), National Key Research and Development Program of China (2022 YFC3602104), Beijing Science and Technology Program (Z211100002921028), Capital's Funds for Health Improvement and Research (CFH2022-2-2025), Special Scientific Research Fund for Tutor (YYDSZX201901) and Tongzhou Science and Technology Program (KJ2023CX016).

Conflict of Interest

The authors declare no conflict of interest.

Supplementary Material

Supplementary material associated with this article can be found, in the online version, at https://www.magonlinelibrary.com/doi/suppl/10.12968/hmed.2024.0585.

References

Balan GG, Arya M, Catinean A, Sandru V, Moscalu M, Constantinescu G, et al. Anatomy of Major Duodenal Papilla Influences ERCP Outcomes and Complication Rates: A Single Center Prospective Study. Journal of Clinical Medicine. 2020; 9: 1637. https://doi.org/10.3390/jcm9061637

Ben Ayed H, Koubaa M, Hammami F, Marrakchi C, Rekik K, Ben Jemaa T, et al. Performance of an Easy and Simple New Scoring Model in Predicting Multidrug-Resistant Enterobacteriaceae in Community-Acquired Urinary Tract Infections. Open Forum Infectious Diseases. 2019; 6: ofz103. https://doi.org/10.1093/ofid/ofz103

Chen PH, Tung CF, Peng YC, Yeh HZ, Chang CS, Chen CC. Duodenal major papilla morphology can affect biliary cannulation and complications during ERCP, an observational study. BMC Gastroenterology. 2020; 20: 310. https://doi.org/10.1186/s12876-020-01455-0

Dusunceli Atman E, Erden A, Ustuner E, Uzun C, Bektas M. MRI Findings of Intrinsic and Extrinsic Duodenal Abnormalities and Variations. Korean Journal of Radiology. 2015; 16: 1240–1252. https://doi.org/10.3348/kjr.2015.16.6.1240

Fukusada S, Shimura T, Iwasaki H, Okuda Y, Katano T, Nishigaki R, et al. Relationship between Immunophenotype and Clinicopathological Findings for Superficial Nonampullary Duodenal Epithelial Tumor. Digestion. 2021; 102: 870–877. https://doi.org/10.1159/000514812

Gaspar J, Shami VM. The role of EUS in ampullary lesions: is the answer black and white? Gastrointestinal Endoscopy. 2015; 81: 389–390. https://doi.org/10.1016/j.gie.2014.11.029

Haraldsson E, Swahn F, Verbeke C, Mattsson JSM, Enochsson L, Ung KA, et al. Endoscopic papillectomy and KRAS expression in the treatment of adenoma in the major duodenal papilla. Scandinavian Journal of Gastroenterology. 2015; 50: 1419–1427. https://doi.org/10.3109/00365521.2015.1046912

Hijikata K, Nemoto T, Igarashi Y, Shibuya K. Extra-ampullary duodenal adenoma: a clinicopathological study. Histopathology. 2017; 71: 200–207. https://doi.org/10.1111/his.13192

Ivanovic AM, Alessandrino F, Maksimovic R, Micev M, Ostojic S, Gore RM, et al. Pathologic Subtypes of Ampullary Adenocarcinoma: Value of Ampullary MDCT for Noninvasive Preoperative Differentiation. AJR. American Journal of Roentgenology. 2017; 208: W71–W78. https://doi.org/10.2214/AJR.16.16723

Jang SY, Kim JS, Baek SY, Lee HA, Lee JK. Proposed nomogram predicting neoplastic ampullary obstruction in patients with a suspected ampulla of Vater lesion on CT. Abdominal Radiology. 2021; 46: 3128–3138. https://doi.org/10.1007/s00261-021-02975-3

Kandler J, Neuhaus H. How to Approach a Patient With Ampullary Lesion. Gastroenterology. 2018; 155: 1670–1676. https://doi.org/10.1053/j.gastro.2018.11.010

Kawashima H, Ohno E, Ishikawa T, Iida T, Tanaka H, Furukawa K, et al. Endoscopic papillectomy for ampullary adenoma and early adenocarcinoma: Analysis of factors related to treatment outcome and long-term prognosis. Digestive Endoscopy. 2021; 33: 858–869. https://doi.org/10.1111/den.13881

Komori S, Kawai M, Nitta T, Murase Y, Matsumoto K, Shinoda C, et al. A case of carcinoma of the papilla of Vater in a young man after subtotal colectomy for familial adenomatous polyposis. World Journal of Surgical Oncology. 2016; 14: 47. https://doi.org/10.1186/s12957-016-0806-8

Li S, Wang Z, Cai F, Linghu E, Sun G, Wang X, et al. New experience of endoscopic papillectomy for ampullary neoplasms. Surgical Endoscopy. 2019; 33: 612–619. https://doi.org/10.1007/s00464-018-6577-2

Lian PL, Chang Y, Xu XC, Zhao Z, Wang XQ, Xu KS. Pancreaticoduodenectomy for duodenal papilla carcinoma: A single-centre 9-year retrospective study of 112 patients with long-term follow-up. World Journal of Gastroenterology. 2017; 23: 5579–5588. https://doi.org/10.3748/wjg.v23.i30.5579

Luchini C, Veronese N, Pea A, Sergi G, Manzato E, Nottegar A, et al. Extranodal extension in N1-adenocarcinoma of the pancreas and papilla of Vater: a systematic review and meta-analysis of its prognostic significance. European Journal of Gastroenterology & Hepatology. 2016; 28: 205–209. https://doi.org/10.1097/MEG.0000000000000520

Mehta NA, Shah RS, Yoon J, O'Malley M, LaGuardia L, Mankaney G, et al. Risks, Benefits, and Effects on Management for Biopsy of the Papilla in Patients With Familial Adenomatous Polyposis. Clinical Gastroenterology and Hepatology. 2021; 19: 760–767. https://doi.org/10.1016/j.cgh.2020.05.054

Meijer LL, Strijker M, de Bakker JK, Toennaer JG, Zonderhuis BM, van der Vliet HJ, et al. Clinical outcomes of patients with duodenal adenocarcinoma and intestinal-type papilla of Vater adenocarcinoma. World Journal of Gastrointestinal Oncology. 2020; 12: 347–357. https://doi.org/10.4251/wjgo.v12.i3.347

Nagtegaal ID, Odze RD, Klimstra D, Paradis V, Rugge M, Schirmacher P, et al. The 2019 WHO classification of tumours of the digestive system. Histopathology. 2020; 76: 182–188. https://doi.org/10.1111/his.13975

Nappo G, Gentile D, Galvanin J, Capretti G, Ridolfi C, Petitti T, et al. Trans-duodenal ampullectomy for ampullary neoplasms: early and long-term outcomes in 36 consecutive patients. Surgical Endoscopy. 2020; 34: 4358–4368. https://doi.org/10.1007/s00464-019-07206-x

Nikolaidis P, Hammond NA, Day K, Yaghmai V, Wood CG, 3rd, Mosbach DS, et al. Imaging features of benign and malignant ampullary and periampullary lesions. Radiographics. 2014; 34: 624–641. https://doi.org/10.1148/rg.343125191

Panzeri F, Crippa S, Castelli P, Aleotti F, Pucci A, Partelli S, et al. Management of ampullary neoplasms: A tailored approach between endoscopy and surgery. World Journal of Gastroenterology. 2015; 21: 7970–7987. https://doi.org/10.3748/wjg.v21.i26.7970

Peng CY, Lv Y, Shen SS, Wang L, Ding XW, Zou XP. The impact of endoscopic ultrasound in preoperative evaluation for ampullary adenomas. Journal of Digestive Diseases. 2019; 20: 248–255. https://doi.org/10.1111/1751-2980.12719

Prenzel KL, Hölscher AH, Drebber U, Bollschweiler E, Gutschow CA, Stippel DL, et al. Extracapsular lymph node spread as a negative prognostic factor of adenocarcinoma of the pancreas and cancer of the papilla of vater. Pancreas. 2014; 43: 64–68. https://doi.org/10.1097/MPA.0b013e3182a44a91

Rejeski JJ, Kundu S, Hauser M, Conway JD, Evans JA, Pawa R, et al. Characteristic endoscopic ultrasound findings of ampullary lesions that predict the need for surgical excision or endoscopic ampullectomy. Endoscopic Ultrasound. 2016; 5: 184–188. https://doi.org/10.4103/2303-9027.183978

Ridtitid W, Schmidt SE, Al-Haddad MA, LeBlanc J, DeWitt JM, McHenry L, et al. Performance characteristics of EUS for locoregional evaluation of ampullary lesions. Gastrointestinal Endoscopy. 2015; 81: 380–388. https://doi.org/10.1016/j.gie.2014.08.005

Sun CH, Li X, Chan T, Peng Z, Dong Z, Luo Y, et al. Multidetector computed tomography (MDCT) manifestations of the normal duodenal papilla. European Journal of Radiology. 2013; 82: 918–922. https://doi.org/10.1016/j.ejrad.2013.01.007

Wang XJ, Ke JL, Xu JX, Zhou JP, Lu YF, Zhou QM, et al. Radiographic Features and Clinical Factor for Preoperative Prediction in the Bulging Duodenal Papilla With Malignancy. Frontiers in Oncology. 2021; 11: 627482. https://doi.org/10.3389/fonc.2021.627482

Wei W, Mo W, Wang N, Li Q. Research and analysis on computed tomography signs and clinical characteristics of chronic duodenal papilla mucositis and duodenal papillary carcinoma. International Journal of Immunopathology and Pharmacology. 2023; 37: 3946320231157868. https://doi.org/10.1177/03946320231157868

Wei X, Chen K, Li DC, Li H, Zhu L, Wang ZG. Risk and Prognostic Factors for Small Bowel Adenocarcinoma: A Multicenter Retrospective Observational Study in China. Clinical Medicine Insights. Oncology. 2022; 16: 11795549221091207. https://doi.org/10.1177/11795549221091207